ATOLL RESEARCH BULLETIN

NO. 197.

CHRISTMAS ISLAND (PACIFIC OCEAN): RECONNAISSANCE GEOLOGIC OBSERVATIONS

by Mark J. Valencia

Issued by
THE SMITHSONIAN INSTITUTION
Washington, D.C., U.S.A.

February 1977

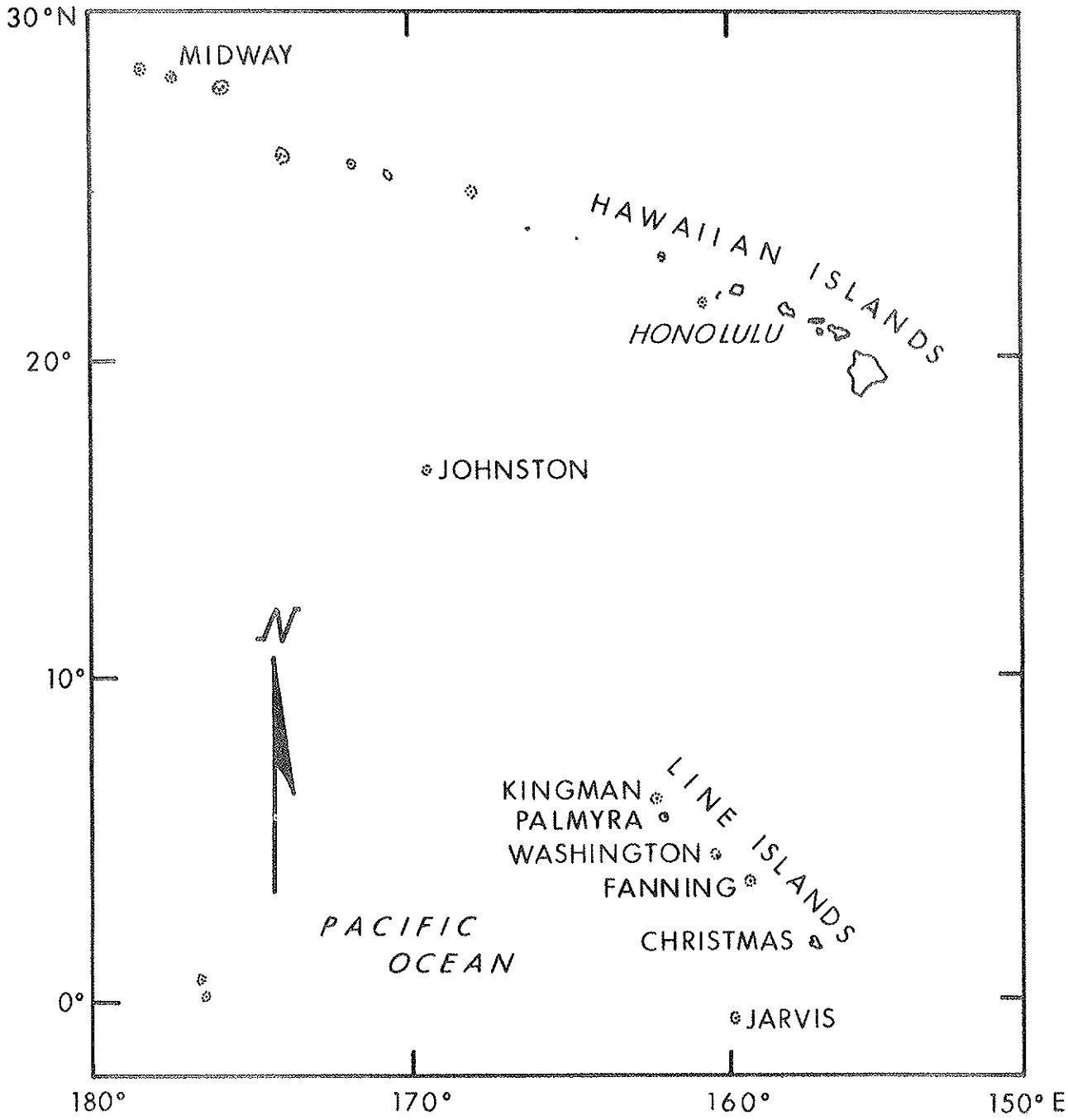

Figure 1. Location of Christmas Island.

Atoll Research Bulletin No. 197. Valencia, M.J. Feb. 1977

CHRISTMAS ISLAND (PACIFIC OCEAN): RECONNAISSANCE GEOLOGIC OBSERVATIONS

by Mark J. Valencia[2]

INTRODUCTION

Christmas Island[3], the largest atoll in the world in terms of subaerial surface area, is located 200 km north of the equator in the equatorial dry zone (Schott, 1933) (Figure 1). The atoll is influenced by nearly constant 4 m/sec easterly winds and an average annual precipitation of 873 mm unevenly distributed in time (Jenkin and Foale, 1968). The shape of this southernmost of the northern Line Islands is like an elongated lobster claw with pinchers open to the northwest containing a semi-circular lagoon (Figure 2). Two passes, each nearly 2 km wide, connect the main lagoon to the ocean. Numerous sub-rectangular shaped hypersaline lakes are found to the east of the main lagoon as well as centrally along the elongated "arm" which extends 18 km to the southeast. Along the southeastern margin of the lagoon, the lakes are more numerous, and narrow channels connect some of them to the lagoon.

Wentworth (1931) and Wentworth and Ladd (1931) have reported reconnaissance observations on the general geology and sediments of Christmas Island, and detailed analysis of landform, soils, and hydrology is included in a report on the coconut-growing potential of the island by Jenkin and Foale (1968). The soils have been further investigated by Hammond (1969). Geologic data gathered by British

---

[1] Hawaii Institute of Geophysics Contribution No. 588.

[2] Hawaii Institute of Geophysics University of Hawaii, Honolulu, Hawaii 96822. Present address: UNDP Regional Offshore Prospecting in East Asia, c/o ECAFE, Sala Santitham, Bangkok 2, Thailand.

[3] First western contact and name courtesy of Captain James Cook, December 24, 1777.

(Manuscript received June 1974 --Eds.)

scientists prior and subsequent to a 1957 nuclear test ("Operation Grapple") (Jenkin and Foale, 1968) conducted at 9,140 m above the southeast point, and by private guano and phosphate rock enterprises at various times, is acknowledged, but such data were for the most part unavailable to the author.

This paper reports 19 days of field observations and subsequent laboratory analysis of samples collected on two expeditions during March and November 1970 which investigated the *Artemia* (brine shrimp) aquaculture potential of Christmas Island. The expeditions were supported by National Sea Grant Program Grant 2-35-243 to P. Helfrich of the Hawaii Institute of Marine Biology, and by private individuals Seymour Gaines and Maurice Rakowicz. The aid of Fred Farrel, Glenn Fredholm, John Hance, and Mayo Ryder during the field investigations is gratefully acknowledged. Preparation of this paper was done while the author was with the Hawaii Institute of Geophysics.

General geology

Christmas Atoll surmounts the southeasternmost portion of a northwest-southeast trending volcanic ridge. The oceanic crust surrounding the ridge exhibits a broad moat and arch, with the arch crest some 240 km distant from the ridge axis. An archipelagic apron forms a smooth curve grading into the insular slope (Menard, 1964). An echo sounder profile of the southwestern slope shows "cone-like" features of probable volcanic origin (Ritchie, 1958). From the reef margin to a depth of 1300 m, the slope is quite steep (Jenkin and Foale, 1968). Coral thickness is 30 m at Motu Tabu (Figure 2) and elsewhere exceeds 120 m (Northrup, 1962; Jenkin and Foale, 1968; John Dryden, oral communication, 1971).

The island can be classified into six subaerial and two submarine landform units (Jenkin and Foale, 1968) on the basis of morphology and sediment type. Table 1 and Figure 3 summarize the geomorphologic characteristics of these landform units. Maximum elevation is 10.7 m above msl in the coastal dune unit along the Bay of Wrecks (Jenkin and Foale, 1968), although masses of reef rock distributed throughout the island's inland area exhibit a rather uniform height not exceeding 4 m above present sea level (Wentworth, 1931).

On the lagoon flats as much as a meter, but more commonly less than 10 cm, of beachrock (biosparudite, Folk, 1965) caps extensive areas of reef rock (coral biolithite and intrasparrudite) and unconsolidated medium calcirudite. Thicker beachrock sections indicating cycles of deposition and beachrock formation are exposed along walls of collapsed spring channels which feed many of the enclosed lakes (e.g., Lakes 16a, 19e, and 27b) and on islet edges within Lake 27a. Incipient beachrock formation was observed in dry areas of Manulu Lagoon and at 30 cm below the floor of an inactive spring channel entering Lake 19e.

In situ *Acropora* and *Tridacna* reef complexes are exposed along some lake margins. Repeated attempts at deep probing of the inter-lake margins betwen Lakes I4 and F7 and on the southeastern shore of 27a met

with an impenetrable horizon at approximately 6.5 m below the surface.

HYPERSALINE LAKES

The approximately 500 isolated and interconnected hypersaline lakes occupying 25 per cent of the total island surface area are of particular interest. In area the lakes range from the 16 km^2 Manulu Lagoon to puddles a few meters wide and centimeters deep (Figure 2). Frequently, differences in water level of a meter of more were observed between adjacent lakes, e.g., the water level of Lake EZ was 1.2 m higher than that of Lake 16A. These differences may be explained by variations in the water budgets of the lakes. Successive rings of shell berms or a border of evaporite crystals, either gypsum and halite or gypsum only, around most lakes indicated higher water levels in the past. Large fluctuations in lake surface area result from water level changes of less than a meter due to the generally shallow and gently sloping configuration of the lake basins. The lakes appeared to be at a relatively low level in their recent history; the expeditions took place during a prolonged drought. Lake levels were occasionally a meter or more below inactive spring channels (e.g., Lake 22), and Manulu Lagoon was observed to be partitioned into smaller interconnected lakes, in contrast to maps constructed by Jenkin and Foale (1968) from aerial photographs taken in the 1950's. Asymmetric basin profiles with recently exposed windward shores indicated active aeolian deposition in some lakes, e.g., in Lakes 27A and 16A.

A reducing environment, as indicated by the odor of hydrogen sulphide, was present immediately below the surface sediment in all lakes sampled. A semidiurnal increase in foam (reported previously by Wentworth, 1931), was observed along the leeward shores of many of the enclosed lakes; in the larger interconnected water bodies, linear patterns of foam extending from leeward to half the lake breadth indicated active Langmuir cells.

The lakes were of two basic types, subevaporite and evaporite, depending on the degree and duration of isolation from the main lagoon and ground water. Lakes actively depositing evaporites could be further classified according to the nature of the evaporite. Key indicators of lake types were bottom morphology, sediment type, and the presence or absence of a red gelatinous alga (S. A. Cattell, personal communication) apparently associated with medium hypersalinity, i.e., in this environment, approximately 200 to 300 o/oo.

Relatively isolated lakes, e.g., 19d, 19e, and 33a, were less than 2 m deep and had salinities greater than 300 o/oo. The lake bottoms were rough as a result of a network of polygonally arranged ridges exhibiting nearly 1 m of relief from ridge top to basin floor. The gypsum and halite crust was only 5 cm thick in Lake 33a and overlay red algae interspersed with halite crystals. A 1-m-wide band lacking evaporites or containing only a thin crust of gypsum indicated relatively low salinity seepage along the lake perimeters. (One could

determine those lakes which were actively receiving shoreline seepage by the presence or absence, in the evaporite ring, of halite crystals which are rapidly dissolved by contact with low salinity water.)

Other evaporitic lakes, e.g., 16a and 27a, had active, relatively low-salinity springs (36-41 o/oo) flowing from collapse features as much as 2 m deep eroded in the hardpan-capped reef rock, usually at the shore nearest the main lagoon. The total input rate of water from the several springs at the northern end of Lake 16a was estimated as less than 0.01 m^3/sec. Continuous long-term flow from one spring in Lake 16a was indicated by the presence of a distinctive, sharp, inverse temperature gradient previously noted by Northrup (1962).

These spring-fed evaporitic lakes, also less than 2 m deep, were characterized by a smooth bottom consisting of a 1-cm thick crust of halite cubes overlying at least 1 m of red algae mixed with halite crystals. Core 16a-1 (Table 2) from the windward shore exhibited a regressive sequence, whereas a longer core (16A-2, Table 3) revealed cyclic variation in sediment type. A core of slightly pebbly, coarse sandy calcareous mud (Folk, 1965) from the windward shore of Lake 27a had a minimum sedimentation rate of 1.8 cm/yr for the past 15 years. This measurement is based on gieger count detection of the 1957 nuclear test horizon at 28 cm below the core top (D. Knutsen and R. Buddemeier personal communication, Figure 4). The sedimentation in this core appeared normal and continuous for this location (Table 4).

Lakes that lacked gypsum and halite deposits, e.g., E, F, and I series, were interconnected by narrow channels to the main lagoon. Channel morphologies for lakes in the F series appeared to represent stages in a developmental cycle. Incipient channel development was possibly occurring between Lakes F6 and F7 as indicated by a 2-m-wide, 20-cm-deep water connection between the two lakes over the beach-rock-capped divide. Perhaps during and after infrequent heavy rain, water of low salinity, undersaturated with respect to calcium carbonate, initiates dissolution of the hardpan while flowing between lakes. After an unusually heavy rain, a rise in water levels in the lakes resulting in submerged interlake boundaries has been observed (George Krasnick, personal communication). Once the crust is weakened, the silt and clay would be eroded by the water flow, leaving a sediment dominated by pelecypod and *Acropora* fragments. A more advanced stage in this process was represented by an inactive channel between F2 and F4. At the F2 end, the beachrock crust was absent along 20 m of channel length and the channel was filled with unbroken pelecypod shells. Once the channel bottom is eroded below the water table (0.5 to 1 m on the lagoon flat, Jenkin and Foale, 1968), extensive widening may occur from groundwater seepage and undercutting, as evidenced by blocks of beachrock several meters in diameter slumped into one of the channels. An example of the next stage of this cycle of channel activity was represented by an inactive channel between F4 and F5. A hypersaline puddle was bounded by a shell shoal at the F4 end and a shell berm at the F5 end. As the water evaporates from the puddle, and by capillary evaporation elsewhere, beachrock will form to stabilize the unconsolidated shells.

Line soundings in Lake F2 recorded depths up to 6 m, and fathometer records indicated submerged isolated patch reefs in the F series lakes (Helfrich, *et al.*, 1973). A salinity increase from the main lagoon edge to the interior of interconnected lake series revealed the probable cause of reef and invertebrate extinction in the lakes farthest from the lagoon. A general salinity increase in a northeast-southwest direction for interconnected lake series reflected the influence of permanent fresh-water lenses in the northeast. For example, springs entering lake Alb had salinities of 24 and 16 o/oo. (Helfrich, *et. al.*, 1973).

Nearshore bottom-sediment type varied considerably in these "open" lakes but the dominant type for F series lakes was a sandy, pebble gravel of pelecypod and *Acropora* fragments. The berms around the lake margins consisted of well-sorted pelecypod and gastropod pebble gravel. In windward nearshore Lake F1a, a core penetrated 16 cm of pink organic "fluff" down to an extinct pelecypod bed. Windward sedimentation or reworking is fairly rapid in these open lakes, as evidenced by ruts partially filled and smoothed by the pink organic "fluff" and aeolian silt. These ruts were made 5 months previously by a landrover used by the expedition.

Lagoon

The rectilinear pattern of patch reefs and concomitant depositional upbuilding extended into the lagoon from the southeastern and eastern margins (Helfrich, unpublished data). The margin of the lagoon was not easily defined in these regions due to complexes of broad tidal flats, peninsulas, reefs, and islands. A maximum lagoon depth of 7 m is approximately equivalent to that of the F lakes. In addition to aeolian deposition, large amounts of fine and medium calcareous debris transported from the seaward leeward shore through the passes results in a buildup of the lagoon floor (Wentworth, 1931). Continuous rapid shoaling of the northern pass is evident from its dredging history (Jenkin and Foale, 1968). In spite of high sedimentation rates, patch reef development is more frequent in sheltered areas, such as along the eastern margin, where the substrate is more stable than elsewhere.

Phosphate

Apatite, identified in the field and subsequently confirmed by X-ray analysis (W. Burnett, personal communication), occurs to a depth of 0.5 to 1 m as peripheral and fracture rinds in a 2-acre outcrop of beveled and severly eroded beachrock situated in the lagoon flat unit in the north near Lake 1B (P, Figure 2). This observation is interesting in relation to Hutchinson's (1950) hypothesis that several thousand years ago, the equatorial rain belt was centered over Christmas Island, i.e., farther south than at present. His hypothesis was based on the supposed present day absence of evidence of phosphatization on relatively dry Christmas Atoll in contrast to the present day occurrence of phosphate rock on wetter islands to the north and south.

However, this one occurrence of phosphate rock does not account for the amount of phosphatization that might be expected from the combination of low annual precipitation and the present and presumably past deposition of 200 tons/yr of guano as estimated from bird populations (Helfrich *et al.*, 1973). Avian Mining Company of Canberra, Australia drilled a test hole to 40 m on Motu Tabu, apparently without encountering commercial deposits of apatite (John Dryden, personal communication).

The curious scarcity of both guano and phosphate rock deposits could be ascribed to bird behavioral patterns and to leaching by occassional heavy rains (Helfrich *et al.*, 1973).

Hypothetical geologic development

Variations of rates and directions of spreading within the oceanic crust emanating from the East Pacific Rise produce zones of crustal weakness. During the formation of the Hawaiian Ridge, volcanism progressed from northwest to southeast along such a zone, so the southernmost volcanically active island of Hawaii is not only the youngest but also the largest. The northwest-southeast structural trend of the volcanically extinct Christmas Island ridge and the large size and position of Christmas Atoll relative to the other Northern Line Island atolls to the northwest evoke a comparison with the evolving Hawaiian Ridge. If a similar mechanism of origin applies to the Christmas Island Ridge, the volcanic complex upon which Christmas Atoll has formed is then the youngest of the northern Line Islands, having developed in early Cenozoic time (Menard, 1964).

The basic shape of an atoll is largely dependant on the morphology of its volcanic basement (Wiens, 1962) but the surficial detail is controlled by sea level fluctuations and climatic and tectonic influences. The irregular shape of Christmas Atoll is probably a result of the arrangement of volcanic peaks similar to those observed on the southwest insular slope. The development of the major geomorphologic features is a result of linear patch reef growth, and a progressive westward and northward infilling of the main lagoon, perhaps aided by slow northwestward tilting of the entire atoll. Roy and Smith (1970) speculate that Fanning Atoll, 320 km to the northwest, has tilted up to the west, whereas the nearest land to the south, Jarvis Atoll, 420 km to the southwest, has a filled lagoon floor 2.5 m above sea level with evaporite crystals in the deepest depressions thus indicating recent emergence (Wiens, 1962).

Wiens (1962) has proposed a hypothetical model of the morphological cycle of an atoll with changing sea level (Figure 5). His lowest reef profile represents the appearance of an atoll at the end of the last low stand of the sea (Wisconsin). At that time the emerged reef, which once had been 100 m higher than the Wisconsin level, was dissolved and mechanically eroded so that only portions of the reef periphery (A) and small lagoon highs (D) remained above sea level. At this stage, the lagoon bottom (C) was at sea level. Also produced was a fringing reef flat (B) with an outer algal ridge and a live reef-front with a well-

developed wave-cut bench and a windward spur and groove system.

During the post-Wisconsin eustatic rise of sea level, a rectilinear pattern of *Acropora* and *Tridacna* patch reefs developed on the immersed lagoon floor of Christmas Island parallel or transverse to northeast and southeast modes of wind direction. At present, easterly winds predominate with a minor mode from the southeast, and linear patch reef development transverse to the easterly mode is occurring in the windward lagoon. However, the pattern of lake margins, presumably underlain by reefs, hints at past northeast and southeast wind modes. Linearly arranged patch reefs oriented downwind or, more rarely, transverse to the main wind direction are present in several atoll lagoons (Wiens, 1962) including a rectilinear pattern in Fanning Atoll lagoon (Roy and Smith, 1970). Linear patch reef development was due possibly to more rapid reef growth in divergences of Langmuir cells or to a rectilinear base of sand dunes developed during the Wisconsin low stand. In the latter scheme, patch reefs would have been less well-developed in the leeward than the windward lagoon due to more extensive bar development nearer the windward sediment source. Differential growth rates of coral and coralline algae between the seaward and leeward reefs, possibly aided by northwestward subsidence, resulted in the northwest passes.

As sea level rose to a maximum 2 m level within the last 5000 years (Fairbridge, 1952, 1961), Christmas Island was almost entirely submerged, although lagoon patch reef development kept pace with the rising sea level. During the brief still-stand and the subsequent eustatic fall of sea level, the reefs were planed off, supplying sediment to the emerging lakes. Beachrock formation on leveled, exposed reef tops incorporated bivalves and other biogenic debris. Aeolian sediment, derived from the emerged windward coastal plain and the seaward beaches, formed the coastal inland and lagoon dunes and also accumulated in the lake basins, along with autochthonous biogenic sediment. Wave transportation and deposition of sediment was effective in plugging breaches in lake peripheries. The lakes progressively filled and became isolated from the main lagoon, although some ephemeral shallow channels were maintained by tidal flow. The increasing salinity curtailed reef and invertebrate growth, and bivalve and gastropod shells accumulated in berms on the leeward lake shores. The windward lagoon is now in the incipient stage of this process of hypersaline lake formation, whereas the interconnected lakes are indicative of the next stage. The completely isolated lakes continue to shoal due to precipitation of evaporites, principally gypsum and halite.

REFERENCES

Fairbridge, R. W., 1952. Multiple stands of the sea in post-glacial times. *Proc. 7th Pacific Sci. Congr.*, 3.

Fairbridge, R. W., 1961. Eustatic changes in sea level. *Physics and Chemistry of the Earth*, 4: 99-185.

Folk, R. L., 1965. *Petrology of sedimentary rocks:* Hemphill's, Austin, Texas, 159 pp.

Hammond, T. T., 1969. *The characterization and classification of the soils of Christmas Island:* Unpublished, Univ. Hawaii M. S. thesis, 109 pp.

Helfrich, Philip, in collaboration with John Ball, Andrew Berger, Paul Bienfang, S. Allen Cattell, Mari Dell Foster, Glen Fredholm, Brent Gallagher, Eric Guinther, George Krasnick, Maurice Rakowicz, and Mark Valencia, 1973. The feasibility of brine shrimp production on Christmas Island. *Univ. Hawaii Sea Grant Tech. Rept.* TR-73-02, 173 pp.

Hutchinson, G. E., 1950. The biochemistry of vertebrate excretion. *Bull. Amer. Museum Nat. Hist.* 96: 1-554.

Jenkin, R. N. and Foale, M. A., 1968. An investigation of the coconut-growing potential of Christmas Island. Ministry of Overseas Development, Resources Division, Directorate of Overseas Surveys, Tolworth, Surrey, England, *Land Resources Study* No. 4, vol. 1.

Menard, H. W., 1964. *Marine Geology of the Pacific.* McGraw-Hill Book Co., London, pp. 79, 92.

Northrop, John, 1962. Geophysical observations on Christmas Island. *Atoll Research Bull.* 89: 1-2.

Ritchie, G. S., 1958. Sounding profiles between Fiji, Christmas and Tahiti Islands. *Deep-Sea Res.*, 5: 162-168.

Roy, K. J. and Smith, S. V.,1970. Sedimentation and coral reef development in turbid water: Fanning Lagoon. *Hawaii Institute of Geophysics Report* HIG-70-23: 61-76.

Schott, G., 1933. The distribution of rain over the Pacific Ocean. *Proc.5th Pacific Sci. Congr.* 3: 1887-1890.

Wentworth, C. K., 1931. Geology of the Pacific Equatorial Islands. *Bernice P. Bishop Museum Occ. Pap.* IX, 15: 3-25.

Wentworth, C. K. and Ladd, H. S., 1931. Pacific Island sediments. *Stud. Nat. Hist. Iowa Univ.*, 13: 1-47.

Wiens, H. J., 1962. *Atoll environment and ecology:* Yale Univ., 532 pp.

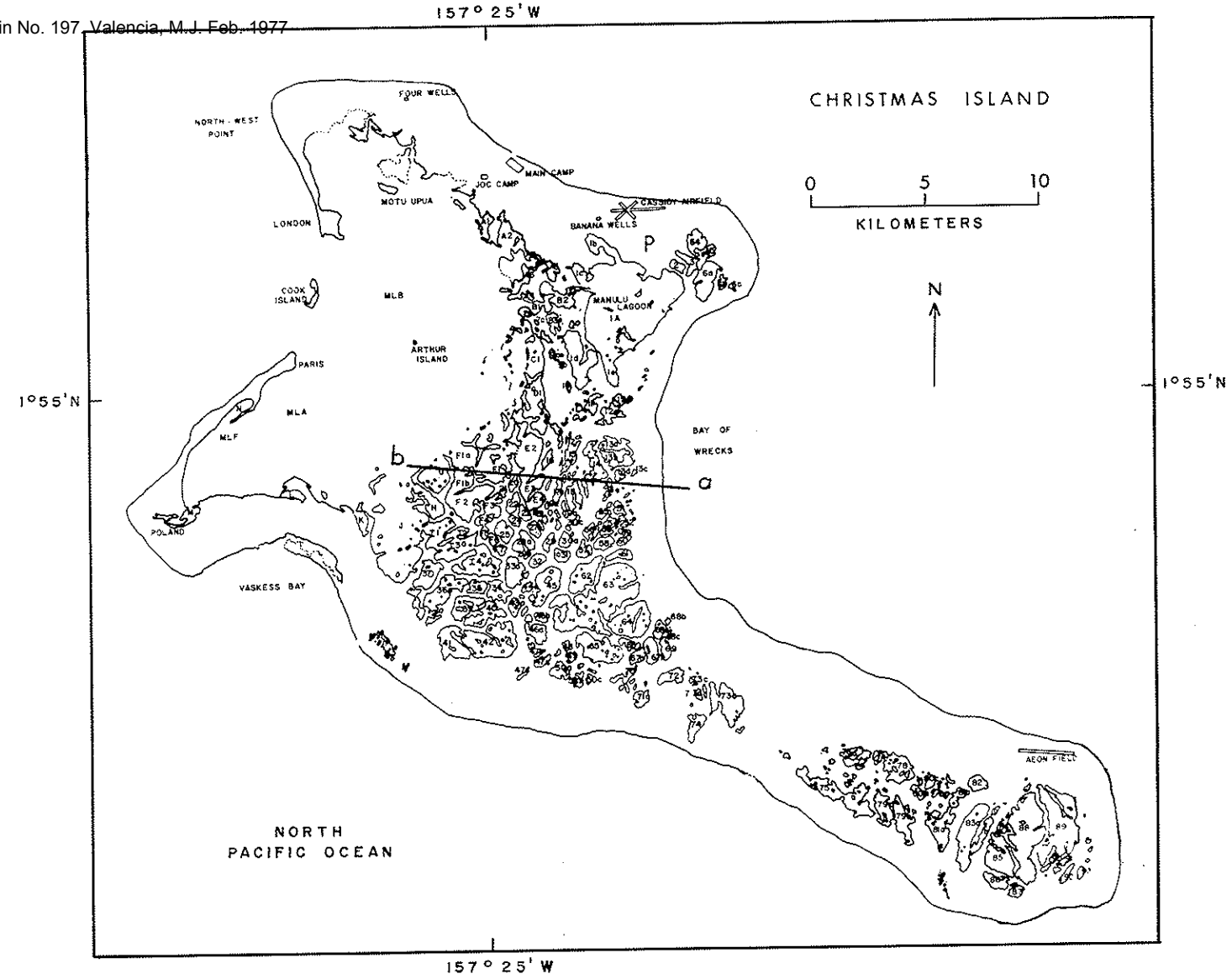

Figure 2. Map of Christmas Island with labels for saline lakes. P is outcrop of phosphate rock (apatite): a---b is line of section in Figure 3.. Letters denote lake series which are connected to the lagoon, and numbers indicate isolated water bodies (from Helfrich *et al.*, 1973).

Table 1. Characteristics of submarine and subaerial landform units of Christmas Island (summarized from Jenkin and Foale, 1968).

Unit	Description
Seaward reef	Platform 30-120 m wide around entire perimeter; widest on northern coast. Groove and spur structure on seaward margin; better developed on leeward (western) coast. Windward coast has algal ridge exposed 50 cm at low tide.
Seaward beach	Leeward beach 6 m wide; windward beach 2 m wide; maximum exceeds 10 m. Leeward beach composed of well-rounded, well-sorted medium coral and mollusk sand. Windward beach is steeper and composed of rounded coral "shingles".
Beach crest, coastal dunes, and boulder rampart	Beach crest is 2 m side, 3-4 m high, coral sand ridge along westernmost end of northern coast and parts of southern coast. Beach crest replaced by extensive coastal dunes up to 50 m wide and 6-10.7 m high along parts of northern coast and southwestern corner of Bay of Wrecks. Coastal dune sand is derived from seaward beach sand. Angular coral boulders 15 to 50 cm in diameter form a rampart up to 30 m wide and 2-3 m high along parts of the Bay of Wrecks and the Southeast Peninsula.
Coastal plain	Plain is 100-200 m wide and consists of coral sand, gravel, and boulders up to 10 cm in diameter. Occasional silted-up or evaporated land-locked lagoons; e.g., lagoon behind Cecile Peninsula.
Central ridge and inland dunes	Represents former coastline; beach sands mechanically similar to seaward beach and aeolian coral sand augmented by organics from nesting sooty terns. Coral fragments up to 10 cm in diameter occur below 150 cm. Central ridge occurs extensively in the north, less extensively near the southern and southwestern coasts, and infrequently in the east and southeast. Central ridge 4 m above mean sea level at New Zealand airfield, augmented by aeolian sand from lagoon flats. North of Poland, central ridge is predominantly derived from aeolian lagoonal flat sand. Central ridge 5 m above mean sea level in north and around Bay of Wrecks; coral sand derived from seaward beach and beach crest. Inland dunes in Four Wells area and Auverne Sandhills in south.

Table 1. (Continued)

Lagoon scarp and lagoon dunes	Scarp is 1 to 1.5-m drop over a 12-m distance between central ridge and lagoon flats; where central ridge absent, no scarp occurs. North of Poland and London, scarp is replaced by line of lagoon dunes on lagoon edge of central ridge; dunes formed from aeolian sand derived from lagoon beach and flats.
Lagoon flat and lagoon beach	Flats less than 1 m above mean sea level enclose hypersaline lakes and border the main lagoon on the north, east, and south; they also occur along the interior of the Southeast Peninsula. Sediment on lagoon flats to the north of the main lagoon and near the Southeast Point is generally fine-to-medium coral sand with coral boulders up to 10 cm in diameter below 30 cm. Hardpan (beachrock) up to 25 mm thick covers lagoon flat on eastern and southern sides of main lagoon and around hypersaline lakes in center of Southeast Peninsula; sediment beneath hardpan similar to uncovered sediment elsewhere in lagoon flats. Near the bathing lagoon and on Motu Tabu, Motu Upua, and Cook Island, coarser coral sand covers the finer lagoonal sediments. Gently sloping beaches composed of finer-to-medium coral sand occur along the western coast of the main lagoon and along the western edge of Manulu and the Isles Lagoon.
Lagoon reef	Moderately well-developed in sheltered eastern main lagoon; patch reefs in western main lagoon. High sedimentation rate and shifting substrate in shallow (7 m depth maximum) lagoon inhibit coral development.

Table 2. Megascopic description of sediments in Core 16a-1.

Depth (cm)	Description
0 - 2	Pebble-size halite crystals in groundmass of green alga-calcium carbonate-halite mud; some pebble-size pelecypod fragments.
2 - 10	Bimodal sediment: whole pebble- and cobble-size gastropod and pelecypod shells in groundmass of sand-size shell fragments.
10 - 16	Coarse sand-size gastropods; rounded and subangular pebble-size shell fragments partially cemented together with calcium carbonate; occasional entire leaves.
16 - 30	Scattered coarse sand-size gastropods in white calcium carbonate mud matrix.
30 - 59	Occasional gastropod and pelecypod fragments in pink calcium carbonate mud matrix.

Table 3. Megascopic description of sediments in Core 16a-2.

Depth (cm)	Description
0 - 4	Brownish-green algal mud; occasional pelecypod fragments.
4 - 9	Brownish-pink algal mud; occasional pelecypod fragments.
9 - 10	Pink algal mud.
20 - 27	Same; abundant gastropod and pelecypod shell fragments and intact pelecypod halves.
27 - 29	Gastropod layer.
29 - 30	Brownish-red algal mud.
30 - 43	Tan-colored algal mud; abundant gastropod and pelecypod shell fragments and whole large gastropods.
43 - 49	Yellowish-brown algal mud.
49 - 58	Light-tan-colored algal mud; abundant sand-size gastropod and pelecypod shell fragments; green algal layer at 52 cm.
58 - 69	Intact pelecypod halves and large gastropods in tan-colored algal mud matrix.
69 - 79	Tan-colored mud; not algal.
79 - 82	Pelecypod and gastropod shell fragment sand.

Table 4. Megascopic description of sediments in Core 27a-1.

Depth (cm)	Description
0 - 6	Sand-size and silt-size gastropod and pelecypod shell fragments partially cemented together with calcium carbonate; occasional benthic foraminifera.
6 - 63	Same; abundant rounded beachrock pebbles with exterior black algal coating.
63 - 120	White calcium carbonate mud with occasional aeolian pebbles.

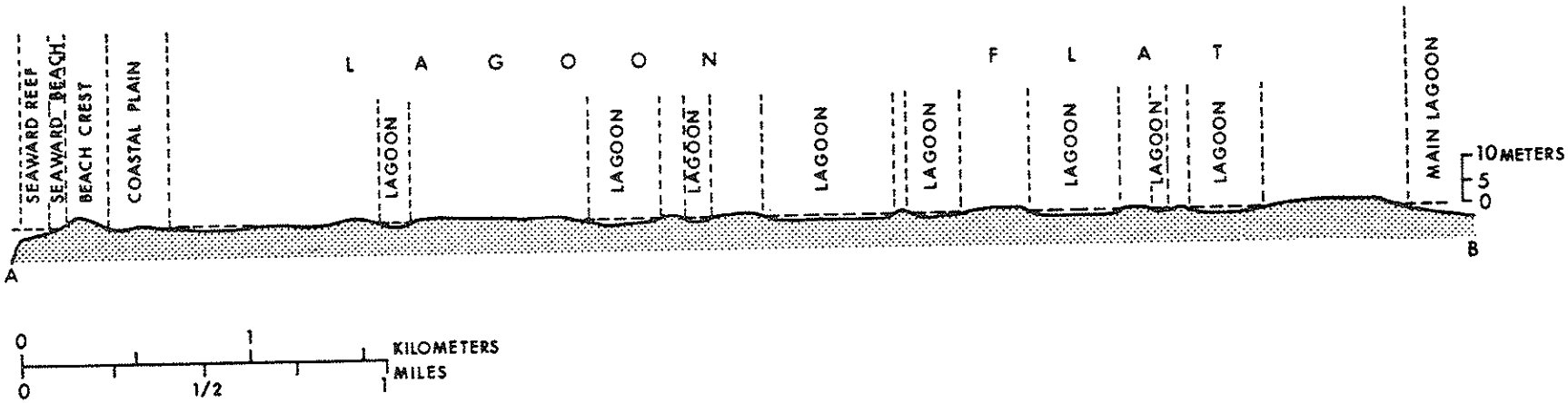

Figure 3. Representative topographic cross-section including the geomorphologic zones outlined in Table 1 (from Jenkin and Foale, 1968).

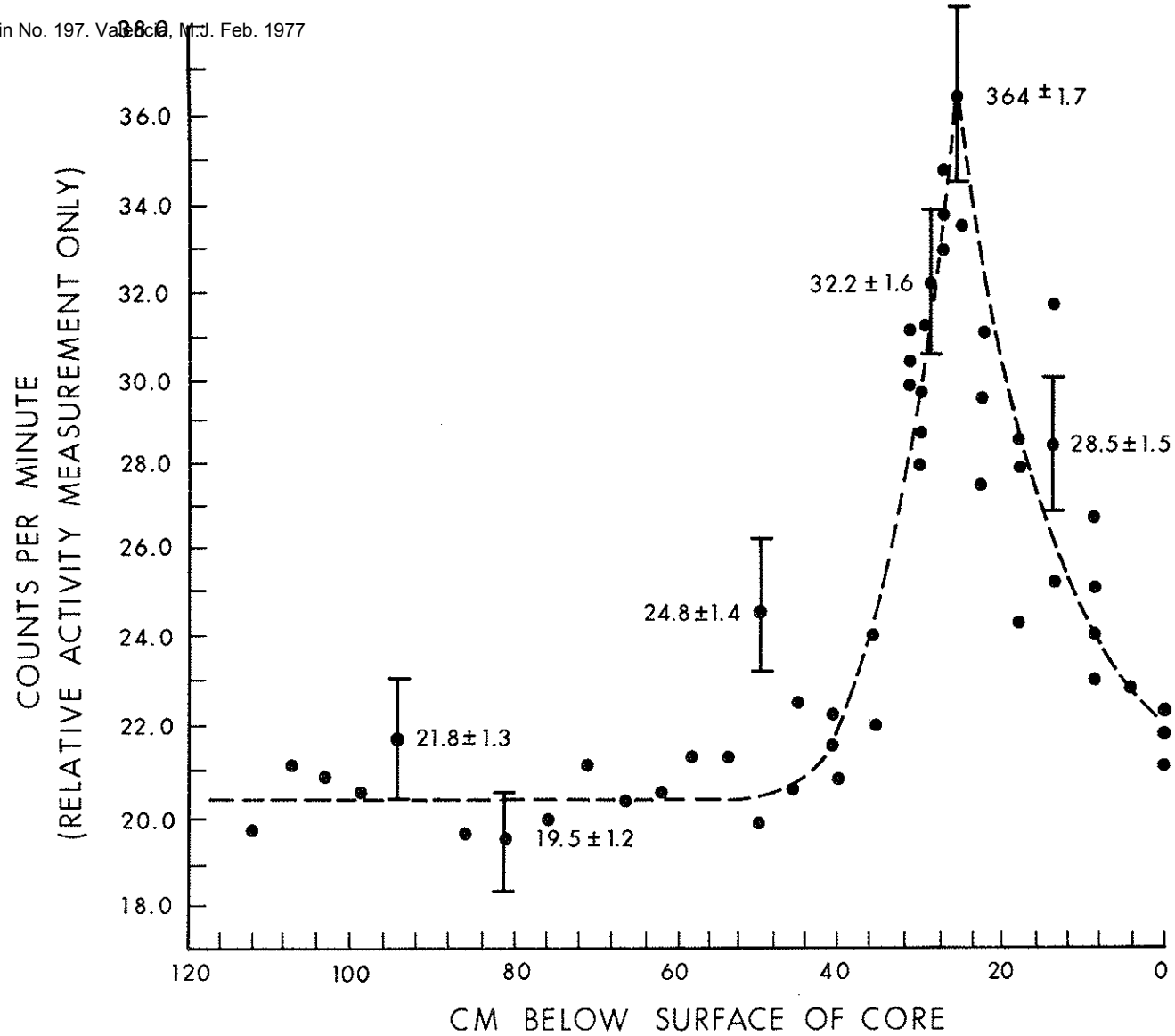

Figure 4. Graph of radioactivity of Core 27a with depth. Bars represent ± 1 standard deviation for selected points. All counting intervals were the same, so equivalent rates have the same standard deviation. The slight deviation from a step function is due to resolution limitations of the 5-7.5 cm-wide detectors; for example, the maximum activity at 28 cm is still detectable at 32 cm. The graph is consistent with a single event and no post-depositional sediment disturbance (after D. Knutsen and R. Buddemeier, unpublished data).

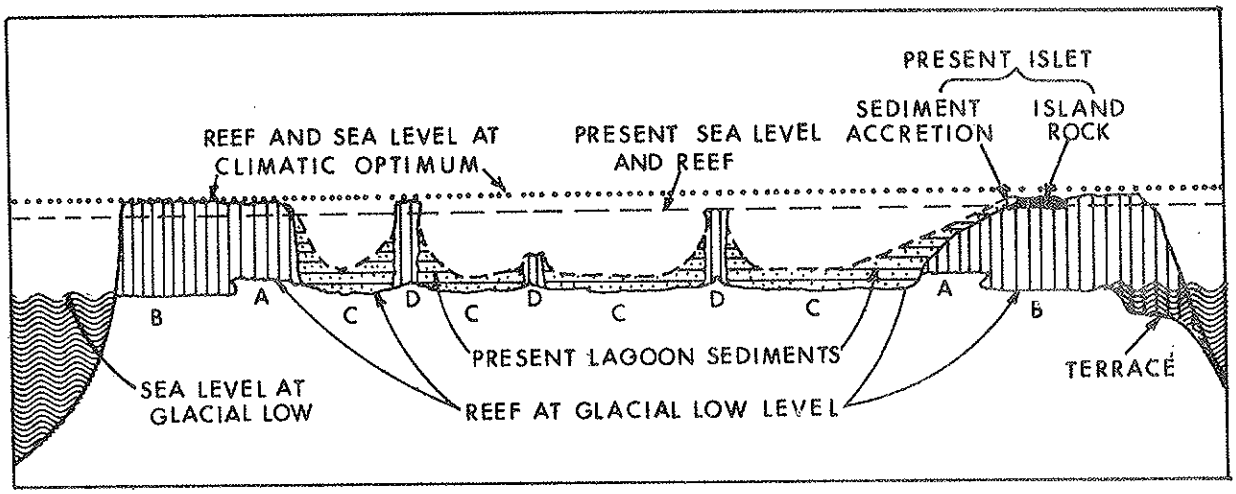

Figure 5. Hypothetical diagram of atoll evolution. A, undercut "raised" reef remnant; B, old reef flat; C, old lagoon bottoms; D, coral patches, knolls, or pinnacles. (From Wiens, 1962, Figure 40.)